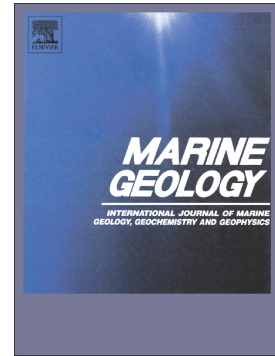


## Accepted Manuscript

Sedimentary processes on the continental slope off Kvitøya and Albertini troughs north of Nordaustlandet, Svalbard – The importance of structural-geological setting in trough-mouth fan development

O. Fransner, R. Noormets, A.E. Flink, K.A. Hogan, J.A. Dowdeswell



PII: S0025-3227(17)30037-3  
DOI: doi:[10.1016/j.margeo.2017.10.008](https://doi.org/10.1016/j.margeo.2017.10.008)  
Reference: MARGO 5704  
To appear in: *Marine Geology*  
Received date: 10 February 2017  
Revised date: 12 September 2017  
Accepted date: 14 October 2017

Please cite this article as: O. Fransner, R. Noormets, A.E. Flink, K.A. Hogan, J.A. Dowdeswell, Sedimentary processes on the continental slope off Kvitøya and Albertini troughs north of Nordaustlandet, Svalbard – The importance of structural-geological setting in trough-mouth fan development. The address for the corresponding author was captured as affiliation for all authors. Please check if appropriate. *Margeo*(2017), doi:[10.1016/j.margeo.2017.10.008](https://doi.org/10.1016/j.margeo.2017.10.008)

This is a PDF file of an unedited manuscript that has been accepted for publication. As a service to our customers we are providing this early version of the manuscript. The manuscript will undergo copyediting, typesetting, and review of the resulting proof before it is published in its final form. Please note that during the production process errors may be discovered which could affect the content, and all legal disclaimers that apply to the journal pertain.

**Sedimentary processes on the continental slope off Kvitøya  
and Albertini troughs north of Nordaustlandet, Svalbard –  
the importance of structural-geological setting in trough-  
mouth fan development**

O. FRANSNER<sup>1\*</sup>, R. NOORMETS<sup>1</sup>, A. E. FLINK<sup>1</sup>, K. A. HOGAN<sup>2</sup>, J. A.  
DOWDESWELL<sup>3</sup>

*<sup>1</sup>Department of Arctic Geology, University Centre in Svalbard,  
Longyearbyen 9171, Norway*

*<sup>2</sup>British Antarctic Survey, Natural Environment Research Council,  
Cambridge CB3 0ET, United Kingdom*

*<sup>3</sup>Scott Polar Research Institute, University of Cambridge, Cambridge CB2  
1ER, United Kingdom*

*\*Corresponding author (e-mail: oscarjacob.fransner@unis.no)*

**Abstract**

New marine-geophysical data were analyzed to investigate the sedimentary processes operating on the continental slope north of Nordaustlandet, Svalbard. Kvitøya Trough terminates in a trough-mouth fan (TMF) on the slope, whereas Albertini Trough incises the shelf edge and a TMF is notably absent. Instead, the continental slope beyond Albertini Trough is dominated by thick, acoustically stratified units likely formed by down-slope and along-slope sedimentological processes combined. The morphological and sedimentological differences between Albertini and Kvitøya troughs may partly be due to the larger dimensions of Kvitøya Trough and its associated glacial

catchment area relative to Albertini, suggesting that the transport of a larger volume of glacial sediments potentially was a contributing factor in building Kvitøya TMF. By contrast, the downfaulted bedrock below outer Albertini Trough provided larger accommodation space for glacial sediments which accumulated in an outer-shelf basin, highlighting the importance of the structural-geological setting in TMF development. Debris-flow deposits and/or channel-levée deposits on the lower continental slope and rise off Kvitøya Trough indicate bypassing of glacial sediments from the shelf to the deep ocean, a process that is likely a result of locally steep slope gradients ( $< 9^\circ$ ). The volume of the Kvitøya TMF is smaller than TMFs along the western Svalbard margin, which may be linked to the more erosion-resistant bedrock of the northern margin and/or the comparatively small drainage basin of Kvitøya Trough compared to drainage basins of ice streams that drained westwards from Barents Sea. In addition, the Kvitøya TMF is incised by gullies indicating that they formed after Last Glacial Maximum (LGM) while larger tributary canyons flanking the Kvitøya TMF likely have developed during a longer time span. High seafloor backscatter values in the tributary canyons and gullies are interpreted as coarse-grained deposits that lead down-slope to debris-flow deposits, suggesting an origin for the tributary canyons and

gullies through incision by gravity flows of sediment-laden meltwater during and/or after deglaciation.

### **Keywords**

Nordautlandet continental slope, sedimentary processes, trough-mouth fan development

### **1. Introduction**

The marine-based Svalbard-Barents Sea Ice-Sheet (SBIS) covered the Barents Sea and Svalbard archipelago during the Last Glacial Maximum (LGM) (Siegert et al., 2001; Svendsen et al., 2004; Hughes et al., 2016). The ice sheet was drained by ice streams that eroded cross-shelf troughs during Quaternary full-glacial conditions (e.g. Ottesen et al., 2005, 2007; Hogan et al., 2010), which significantly shaped the morphology of the shelf edge and the adjacent continental slope (e.g. Vorren et al., 1988; Batchelor and Dowdeswell, 2014). The largely diamictic sediments delivered by fast-flowing ice streams to the shelf edge are most often found as stacked glacial debris-flows on the continental slope, forming trough-mouth fans (TMFs) (e.g. Laberg and Vorren, 1995; Ó Cofaigh et al., 2003). The glacial morphology of the continental slope beyond cross-shelf troughs can therefore provide information regarding ice-sheet dynamics and glacial history (e.g. Laberg and Vorren, 1995; Ó Cofaigh et al., 2003). However, several Arctic cross-shelf troughs lack TMFs (c.f. Batchelor and Dowdeswell, 2014).

This is often attributed to low input of glacial sediments to the shelf edge or to sediment-bypassing of the upper slope (Batchelor and Dowdeswell, 2014). Relatively low fluxes of glacial sediment have been suggested to depend on factors such as bedrock resistance to erosion, relatively small ice-drainage basin area (Ottesen and Dowdeswell, 2009), or to limited ice streaming over the shelf (c.f. Batchelor and Dowdeswell, 2014).

Several TMFs have been described along the western continental margin of Svalbard and the Barents Sea: the Kongsfjorden, Isfjorden, Storfjorden and Bear Island TMFs (e.g. Laberg and Vorren, 1996; Elverhøi et al., 1997; Andreassen et al., 2008; Sarkar et al., 2011). However, on the northern continental margin of Svalbard much less is known about continental slope morphology and its connection to ice-sheet dynamics. There is clear evidence that the SBIS reached the northern shelf edge during the LGM (Knies et al., 2001; Chauhan et al., 2016a) and that Hinlopen Trough was a major drainage pathway for the SBIS that brought ice and sediments to the continental shelf edge (Batchelor et al., 2011). Ice streams are also shown to have occupied Albertini and Kvitøya Troughs, but little is known of the geomorphology and sedimentary processes on the continental slope beyond these two troughs (Figs 1a-b and 2a) (Hogan et al., 2010; Noormets et al., 2012).

In this paper, we investigate the morphology and sedimentary architecture of the continental slope beyond the Albertini and Kvitøya glacial troughs north of Svalbard, and link this to sedimentary processes on the continental slope and past SBIS dynamics on the adjacent shelf. This is addressed using a variety of high-resolution marine-geophysical data including airgun seismic profiles, chirp sub-bottom profiles, and multibeam-bathymetric and backscatter data. By interpreting these data we identify the glacial-sedimentary processes shaping this continental margin, and how and why the margin differs from the western Barents Sea. Ultimately we are contributing to the understanding of the dynamics of the northern SBIS during the last glacial-deglacial cycle.

## **2. Geological and glaciological setting**

The northern continental margin of Svalbard is located in the northwestern Barents Sea (Figs 1a and 2a). It is bounded by the Svalbard archipelago to the south, the Yermak Plateau to the northwest, and the Nansen Basin of the Arctic Ocean to the north. The Barents Sea region consists of a series of platforms and basins that drifted to their present positions from about 20°N in the Carboniferous period through 55°N in the Triassic period (Worsley and Aga 1986; Heafford, 1988; Doré, 1995). Long-term palaeoclimatic factors linked to plate drifting therefore played an important role in determining sedimentary environments in the Barents Sea, which have changed from

carbonate-dominated to clastic deposits with the northward motion of the region (e.g. Gee et al., 2008). Intracontinental sedimentation dominated in the Barents Sea from approximately 240 to 60 Ma before the opening of the Norwegian-Greenland Sea (Doré, 1995; Faleide et al., 1996); however, marine sedimentation has dominated since the late Paleozoic (Heafford, 1988; Doré et al., 1995). However, although the bedrock of Spitsbergen is dominated by sedimentary rocks, Late Precambrian crystalline rocks of Hecla Hoek formation is likely dominating the northern Svalbard margin (Elverhøi and Lauritzen, 1984).

The continental margin around Svalbard has been reshaped significantly by glacial-interglacial processes during the Plio-Pleistocene (e.g. Mangerud et al., 1998). The fjords and troughs of northern Svalbard, such as Wijdefjorden, Rijpfjorden and Hinlopen and Kvitøya troughs demarcate former drainage pathways of the SBIS (Ottesen et al., 2005, 2007; Hogan et al., 2010; Batchelor et al., 2011; Fransner et al., 2017) (Fig. 2a). The erosion rate of streaming ice were probably partly controlled by the underlying bedrock, where high resistance to glacial erosion as found along the northern Svalbard margin probably minimized the local erosion rate there (e.g. Hogan et al., 2010).

Kvitøya Trough has approximate dimensions of  $190 \times 25 \times 0.5$  km (length $\times$ width $\times$ max depth) and a glacial drainage basin

estimated to be around 15,000 km<sup>2</sup> (Fig. 2a) (Dowdeswell et al., 2010). The corresponding dimensions for the smaller Albertini Trough are approximately 100 × 35 × 0.22 km with a drainage basin of approximately 6,000 km<sup>2</sup> (Fig. 2a) (Batchelor and Dowdeswell, 2014).

The beginning of deglaciation after the LGM is dated to c. 18.5 cal. ka BP for the continental shelf edge north of Svalbard (Knies et al., 2001; Chauhan et al., 2016a). Ice-rafted debris (IRD) on the continental slope and significant numbers of iceberg ploughmarks on the continental shelf north of Nordauslandet suggest that calving was of importance during regional deglaciation (Dowdeswell et al., 2010; Hogan et al., 2010; Noormets et al., 2012; Chauhan et al., 2016a; Dowdeswell and Hogan, 2016). Unconsolidated subglacial-deglacial-postglacial sediments are often draped on top of bedrock in the Barents Sea, although sediment thicknesses are variable (Elverhøi et al., 1989). The three typical lithofacies covering bedrock in the NW Barents Sea are, from bottom to top: (1) diamicton, (2), pebbly mud and (3) massive mud (Elverhøi et al., 1989). Radiocarbon dates from above the diamicton on the shelf return deglacial-postglacial ages (Elverhøi et al., 1989). Sediments of LGM and older age, up to c. 74 ka, have, been preserved on the upper continental slope of the northern Svalbard margin (Chauhan et al., 2016a).

The modern oceanography of the northern continental margin of Svalbard is influenced strongly by the West Spitsbergen Current (WSC), which is subdivided into the Yermak and Svalbard branches (e.g. Slubowska et al., 2005) (Fig. 1a). These branches are the main suppliers of relatively warm, Atlantic water into the Arctic Ocean (e.g. Slubowska et al., 2005). The Svalbard branch, due to its flow along the continental margin north of Svalbard, is also of importance for the reworking and redistribution of the unconsolidated sediments there (Slubowska et al., 2005; Vanneste et al., 2006; Chauhan et al., 2016a; 2016b).

### 3. Data acquisition and methods

Air-gun seismic and chirp acoustic shallow sub-bottom profiles, a sediment gravity core, and the majority of the multibeam-bathymetric data used for this study were acquired by the R/V *Helmer Hanssen* in September 2011 and 2013 (Fig. 1c). The seismic data were acquired using a Delph single airgun system with a 30-m long streamer. The chirp acoustic data were collected with a hull-mounted Edge Tech 3300 chirp sub-bottom profiler with a frequency range of 2-16 kHz. A Kongsberg EM300, 30 kHz multibeam echo-sounder system was used to acquire the bathymetric data. Additional multibeam-bathymetric data were acquired by the RRS *James Clark Ross* in 2006 using a Kongsberg EM12, 12 kHz

multibeam system and were provided by the Scott Polar Research Institute, University of Cambridge, UK (Fig. 1c).

The multibeam-bathymetric data were processed, gridded and visualized in the QPS Fledermaus suite. The data were then gridded using a 40 m isometric grid-cell size. Maps of the bathymetric data were produced in ArcMap (version 10.1).

For the sub-bottom data, two-way-travel time (TWT) was converted to depth using a sound velocity of 1500 m/s, which has been used in previous work on shallow glacial-marine sediments (e.g. Hogan et al., 2011; Hjelstuen et al., 2013). Where possible, acoustic units identified on the chirp profiles were correlated with lithological units in sediment gravity core HH11-09 (Fig. 1b). Sedimentological and paleoceanographic analysis of the core can be found in Chauhan et al. (2016a, b).

The majority of the chirp profiles were converted to SEG-Y format for display and analysis in Kingdom Suite (version 8.8). However, some chirp profiles lost resolution during conversion and were kept in their native format (.jsf) for display and analysis in Edgetech Discover 2.0. A sound velocity of 1500 m/s was used to convert the TWT to meters.

The airgun profiles were converted to SEG-Y format for display and analysis in Kingdom Suite (version 8.8). The airgun profiles were analysed in the time domain (i.e. TWT) due to lack of a velocity model for the data. However, an

approximate depth conversion was performed using a sound velocity of 1500 m/s in order to facilitate comparison with the chirp data.

#### **4. Seismic-reflection data: architecture of the continental shelf edge and slope**

##### *4.1 Description*

Seismic-reflection data from the continental shelf edge and slope were already presented by Geissler and Jokat (2004) (Fig. 3). Although their data penetrate deeper than the new data presented here, our data bring new information regarding seismic units and architecture. The total sediment thickness imaged by the seismic-reflection data presented here varies from 0.3 sec TWT (c. 225 m) on the upper continental slope to 0.8 sec TWT (c. 1200 m) on the middle-lower continental slope beyond Albertini Trough (Figs. 4-5).

No seismic units or interpretations were characterized from the continental slope beyond Kvitøya Trough due to the comparatively low quality of the data from there (Fig. 5a).

The sedimentary architecture of the continental slope off Kvitøya and Albertini troughs is characterized by five seismic units (A1-A5) (where “A” stands for “Airgun”) (Table 1). The acoustic characteristics of these units are described in Table 1.

Where visible, the internal reflectors of A1 are semi-parallel to parallel to each other (Table 1). The low amplitude of the reflectors together with the absence of the base of A1 is likely due to loss of the airgun signal due to attenuation with depth. A1 is present on the continental slope beyond Albertini Trough (Fig. 5a). On the middle continental slope between c. 2.18 and 2.3 sec TWT, A1 displays an erosional boundary (Fig. 5d). The sediment stratigraphy immediately to the north of the erosional boundary displays a more chaotic structure (Fig. 5d). A1 is depth-correlated to late-Pliocene sediments interpreted by Geissler and Jokat, (2004) (Fig. 3).

Unit A2 is up to 0.2 sec TWT thick and lies conformably on top of A1 (Fig. 5a). A2 is depth-correlated to lower Quaternary Sediments, as interpreted by Geissler and Jokat, (2004). The erosional boundary in A1 is also visible in A2 (Fig. 5d). The erosional boundary is therefore present between c. 2.0 and 2.3 sec TWT in the stratigraphy at the middle continental slope off Albertini Trough (Fig. 5d).

The internal reflectors of unit A3 generally go from sub-parallel at the upper slope to parallel at the middle to lower slope (Fig. 5b). A3 lies conformably on top of A2 (Fig. 5b) and is depth-correlated to Quaternary sediments (Fig. 3). A3 displays an erosional boundary between c. 1.75 and 1.90 sec TWT on the middle continental slope off Albertini Trough (Fig. 5d).

A4 has several internal reflectors of high amplitude (Table 1). These reflectors generally go from semi-parallel at the upper slope to parallel on the middle to lower slope (Fig. 5b). Local areas of high amplitude and chaotic reflector patterns occur above areas of acoustic blanking (Table 1; Fig. 5d). A4 is generally found conformably on top of A3 (Fig. 5d). A4 is depth-correlated to Quaternary sediments (Fig. 3).

The upper bounding reflector of Unit A5 is of moderate-high amplitude and continuity (Table 1). Its internal reflectors have sub-parallel to chaotic geometries defining lense-shaped units of seismically homogenous to chaotic character. A5 forms hummocky units at the seafloor that dominate the seismic stratigraphy on the continental rise and lower slope beyond Kvitøya Trough (Fig. 6). The hummocky units are present from ca. 3.40 to 3.65 sec TWT, and are depth-correlated to Quaternary sediments following Geissler and Jokat (2004) (Figs. 3, 6).

#### *4.2 Interpretation*

The sub-parallel to parallel reflectors in Unit A1 are probably a result of rhythmical variations in sedimentation (e.g. Hjelstuen et al., 2013). Such variations on continental slopes often consist of alternating clay and sandy silt that are deposited and reworked by down-slope-turbidity and along-slope contour currents (Rebesco et al., 1996; Pudsey, 2000; Dowdeswell et

al., 2006). Although a glacial origin for the sediments cannot be excluded, it is suggested that the majority of the sediments of A1 were deposited by along-slope currents, possibly the WSC, which has formed similar contouritic deposits along the western Svalbard margin (e.g. Rebesco et al., 2013). However, the oldest recorded influx of warm Atlantic water along the northern Svalbard margin is from MIS 6, which is much younger than unit A1 (Knies et al., 2000). It is not possible to confirm here whether unit A1 was deposited by the WSC or by older continental slope processes.

Units A2-A4 have similar seismic-reflector characteristics to A1, which could indicate similar depositional environments. However, the local semi-parallel reflectors in A3 and A4 on the upper slope may indicate a higher energy sedimentary environment with less processes sorting and redistributing the sediments there compared to further downslope. The depth correlation to Quaternary sediments suggests that units A2-A4 were deposited in a glacimarine environment which presumably increased sediment fluxes to the continental slope, at least periodically as ice sheets expanded and retreated across the shelf (Geissler and Jokat, 2004).

The erosional contact affecting both A1 and A2 between c. 2.0 and 2.2 sec TWT is interpreted as a slide scar resulting from a sediment failure at the middle continental slope off Albertini Trough. The part of the sediment stratigraphy to the north of

the slide scar is interpreted as a part of the sediment deposition from the failure due to its chaotic acoustic character (e.g. Garcia et al., 2012) (Fig. 5d).

The erosional boundary in A3 is not connected to the slide scar affecting A1 and A2 (Fig. 5d). Therefore the erosional boundary in A3 is interpreted to have formed by another process than the sediment failure in A1 and A2. The lack of sediment deposition related to the erosional boundary in A3 may indicate that the eroded sediments were transported further from its source. We therefore suggest that A3 was eroded by gully incision (Fig. 5d).

The local high-amplitude and chaotic reflectors in unit A4 are interpreted as local debris-flow deposits (Fig. 5d), which commonly give a chaotic reflector-pattern (e.g. Garcia et al., 2012).

Chaotic reflector geometry of sediment located beyond trough mouths are commonly interpreted to be composed of glacial debris-flow deposits (e.g. Garcia et al., 2012). Unit A5 is therefore interpreted as glacial debris-flow deposits originating from relatively rapid sediment delivery and down-slope transport of sediments by ice streaming to the mouth of Kvitøya Trough during full-glacial times. Since A5 is exclusively present below Kvitøya Trough, A5 cannot be put into relation with the stratigraphy off Albertini Trough where

units A1-A4 are present. However, the different hummocky units building unit A5 as well as the relatively high height of A5 are characteristics often associated with channel-levee deposits formed by sediment overspill along the sides of channels (Kane et al., 2010). Channel-levee deposits are therefore an alternative interpretation for unit A5 (Fig. 6).

## **5. Chirp sub-bottom data: uppermost sediment stratigraphy**

### *5.1 Description*

Eight units named C1-C8 (where “C” stands for “Chirp”) were distinguished in the acoustic stratigraphy (upper c. 50 m of seafloor sediments) from the continental slope (Figs 7-8 and Table 2). The acoustic characteristics of these units are presented in Table 2.

C1 constitutes the acoustic basement and is overlain by units C2-C7 offshore Albertini Trough. Here, C1 shows a tendency of lobate geometry (Fig. 7b). C1 crops out on the continental slope beyond Kvitøya Trough (Figs 7-8). C2 is found conformably on top of C1 on the upper slope beyond Albertini Trough (Fig. 7b). C2 has a maximum thickness of 6 m (Fig. 7b). The maximum thickness of C3 is c. 4.5 m (Fig. 7b). C3 lies conformably on top of C2 (Fig. 7b). C4 is present conformably on top of C3. C4 reaches 3 m in thickness (Fig. 7b). The maximum thickness of C5 is c. 11 m. C5 is present

conformably on top of C4 on the upper slope off Albertini Trough (Fig. 7b). Units C1 to C5 correlate with the top c. 10 m of airgun unit A4 on the upper continental slope off Albertini Trough.

Unit C6 covers the top of the acoustic stratigraphy at the middle and lower slope off Albertini Trough (Fig. 8a). Where present, C6 correlates to the top 50 m of the airgun unit A4 (Fig. 5d). The upper surface of C6 is characterised by V-shaped incisions and internal reflectors are truncated (Fig. 8a). While some of the v-shaped incisions are filled with sediment, others are empty (Fig. 8a). Unit C7 locally overlies C1 on the slope beyond Kvitøya Trough (Fig. 8b). The maximum thickness of C7 is c. 9 m (Fig. 8b). Unit C8 is exclusively present on the continental shelf edge (Table 2). The thickness of C8 cannot be determined due to the very little to no penetration of the acoustic signal below the upper bounding reflector of C8 (Table 2).

### *5.2 Interpretation*

Unit C1 is interpreted as the acoustic basement, consisting of coarse-grained glaciogenic sediments based on little-to-no acoustic penetration of the unit (e.g. Batchelor et al., 2011) (Table 2). The lobate geometry of unit C1 off Albertini Trough could indicate deposition through debris flows there (Fig. 7).

The acoustic transparency and conformable geometry of Unit C2 is typical for relatively homogenous glaci-marine muds deposited through suspension settling, where internal reflectors are likely to be coarser-grained sediments that settle from the water column and deposit as rain-out blankets (cf. Cai et al., 1997) (Table 2).

The top of Unit C3 was sampled by gravity core HH11-09 (Fig. 7b). The correlated core interval consists of mud with relatively thin sand layers towards its base (Chauhan et al., 2016a). The thin sand layers are suggested to cause the internal reflectors of low amplitude and low continuity in this unit. C3 has similar acoustic characteristics as C2, suggesting similar depositional environments for these units (Table 2).

Unit C4 is partly correlated with a reworked sand layer that was deposited c. 24-23 ka cal yr BP (Chauhan et al., 2016a) (Fig. 7b). This unit was interpreted to be of subglacial origin and was deposited on the continental slope through gravity driven processes during the maximum extent of the SBIS (Chauhan et al., 2016a). It is however unlikely that the interpretation of the sand layer in HH11-09 can be extrapolated to the whole C4 unit. Even if C4 contains sand it is likely that this unit just like unit C3 has a mud matrix.

Unit C5 correlates with homogenous muds in core HH11-09; two dates from this unit give ages of 15 ka cal yr BP and 16.9

ka cal yr BP, respectively (Fig. 7b), which are postglacial ages (Chauhan et al., 2016a).

The acoustically stratified character of Unit C6 is interpreted to result from rhythmical variations in sedimentation on the slope (Table 2) (Hjelstuen et al., 2013). On continental slopes such sediments often consist of alternating sandy silts and clays deposited and reworked by down-slope turbidity currents and along-slope contour currents (Rebesco et al., 1996, 2013; Pudsey, 2000; Dowdeswell et al., 2006).

Lens-shaped, acoustically transparent lobes on high-latitude continental slopes are commonly interpreted as debris-flow deposits consisting of glacial sediments (e.g. King et al., 1998; Dowdeswell et al., 2006), and we maintain that interpretation for Unit C7. The glacial sediments that are building unit C7 are therefore interpreted to be derived from an ice stream in Kvitøya Trough during the LGM. These sediments were transported efficiently down-slope to the continental rise rather than simply accumulating on the slope (Fig. 8b).

Unit C8 is interpreted as diamicton based on the little to no acoustic penetration of the unit. Its V-shaped scours are interpreted as iceberg-keel ploughmarks which are almost ubiquitous on the continental shelf north of Nordaustlandet to a depth of 300 m (Dowdeswell et al., 2010; Hogan et al., 2010;

Noormets et al., 2012; Dowdeswell and Hogan, 2016). Support for this interpretation comes from the characteristic V-shaped depressions on shallow-acoustic profiles which are easily correlated with iceberg ploughmarks identified on the multibeam-bathymetric data.

## 6. Multibeam-bathymetric morphological data

The continental shelf edge north of Nordaustlandet is present at a water depth between approximately 200 and 290 m with the deepest areas (250-290 m) at the mouth of Kvitøya Trough (Fig. 1b). The gross morphology of the Albertini and Kvitøya trough mouths shows significant differences in planview: the mouth of Albertini Trough incises into the shelf whereas the mouth of Kvitøya Trough protrudes northwards (Fig. 1b). The geometry of the continental slope beyond the two troughs also shows significant morphological differences. The slope beyond Kvitøya Trough has a concave long-profile shape with a maximum dip of  $9^\circ$  before it reaches the continental rise at a depth of about 3000 m (Fig. 1d). In contrast, the continental slope beyond Albertini Trough is more complex. Down to a water depth of 1000 m the continental slope is comparatively flat, with a maximum dip of  $3-4^\circ$  (Fig. 1d). From 1000 m to the continental rise the slope gradient steepens to a maximum of  $12^\circ$ . Overall, this gives a convex-shaped slope profile (Fig. 1e). Taken together, the study area comprises several morphological features described below.

### 6.1 Trough-mouth fan (TMF)

The Kvitøya TMF is demarcated by depth contours bulging outwards from the shelf edge in water depths between about 300 and 2700 m (Figs 9a and 9e). However, we infer that the down-slope extent of the Kvitøya TMF continues beyond the limits of our dataset because the IBCAO regional bathymetry (Jakobsson et al., 2012) shows that the hummocky terrain of the continental rise continues to the north (Fig. 1b). Taking this area of hummocky terrain into account, we estimate the area of the Kvitøya TMF to be at least 2500 km<sup>2</sup> (Fig. 1b) with an average thickness of Quaternary deposits of 0.53 sec TWT, equivalent to 0.4 km. This yields an estimated volume of approximately 1000 km<sup>3</sup> for the Kvitøya TMF. This volume is relatively small compared to selected TMFs in Table 3 (c.f. Batchelor and Dowdeswell, 2014 and references therein). Although Albertini Trough lacks a TMF, it is possible to estimate the Quaternary deposits in the trough mouth above the downfaulted bedrock. The downfaulted bedrock covers a distance of c. 58 km of the outermost Albertini Trough (Fig. 3b). The width of Albertini Trough is c. 35 km (Table 3). The average thickness of Quaternary deposits in the downfaulted area of Albertini Trough is c. 0.5 sec TWT, equivalent to 0.38 km (Fig. 3b). This gives an estimated volume of 770 km<sup>3</sup> for the Quaternary deposits above the downfaulted bedrock in

Albertini Trough, which is relatively similar to the estimated volume of the Kvitøya TMF.

The multibeam-bathymetric data from Kvitøya TMF indicate that there are large, numerous debris-flow deposits and/or channel-levee deposits that cross-cut each other at water depths between 1900 and 2800 m, indicating multiple down-slope transport events (Fig. 9a). The dimensions of these deposits vary from c.  $8 \times 2 \times 0.1$  km to c.  $16 \times 7 \times 0.1$  km (lengths  $\times$  widths  $\times$  depths; Fig 9a). The debris-flow deposits and/or channel-levee deposits are acoustically chaotic and correlate with seismic unit A5 on the continental rise-lower slope and acoustic unit C7 at the middle slope (Figs. 6; 8b). Although debris flows deposits and channel-levee deposits are formed by different processes, the chaotic nature of the sea bed of the continental rise off Kvitøya Trough makes it difficult to distinguish which of the two processes was the dominating one (Fig. 9a). However, the presence of acoustic unit C7 on the lower slope indicates that debris-flow deposits dominate there (Fig. 8b).

The extent of Kvitøya TMF is also well-defined in seafloor multibeam backscatter data (Fig. 9c). Backscatter returns over the fan have relatively high values (-20 to -30 dB) compared to adjacent slope areas (-30 to -40 dB), although the shelf edge and the debris-flow and/or channel-levee deposits on the lower

continental slope and rise have the highest values (c. -20 to -25 dB).

## **6.2 Slide scar and associated sediment deposit**

An along-slope-elongated slide scar with approximate length of 23.6 km and width of maximum 800 m (in the bathymetry) is located along the middle continental slope where the western tributary canyon system begins (Fig. 10a). The steepest wall of the northwards dipping slide scar is c. 12°. The slide scar correlates to the location of the slide scar visible between 2.0 and 2.2 sec TWT in the seismic-reflection data (Fig. 5c). A lobe-shaped sediment deposit that is elongate in a down-slope direction is located just north of the eastern side of the slide scar (Figs 10a-10b). The lobe-shaped sediment deposit has approximate dimensions of 20×5.5×0.2 km (Figs 10a-10b).

## **6.3 Tributary canyons and gullies**

The multibeam-bathymetric data indicate that V-shaped tributary canyons flank the western and eastern sides of Kvitøya TMF between c. 1160 and 2900 m water depth (Fig. 9a). In addition, the IBCAO map indicates that the slope immediately to the west of the study area also is dissected by similar tributary canyons (Fig. 1b). Here we describe only the tributary canyons to the west and east of Kvitøya TMF that are imaged by our multibeam-bathymetric data, which will be

referred to as the western and the eastern tributary canyon sets, respectively (Fig. 9a).

The western tributary canyon set consists of multiple tributaries located beyond the Albertini trough mouth (Fig. 9). These tributaries have widths and depths between 3000-7000 m and 150-500 m, respectively (Fig. 9d). A channel on the upper continental slope beyond Albertini Trough is connected to the start of the western tributary canyon set (Fig. 9c). The start of the western tributary canyon set correlates to the slide scar in the bathymetry as well as to the erosional boundary of A3, supporting the interpretation of that boundary as formed by canyon incision after the sediment failure on the middle continental slope that formed the slide scar with associated lobe-shaped sediment deposit (Figs 5d and 10a). The sides of the lobe-shaped sediment deposit are eroded by a canyon to the west and smaller gullies to the east (Fig. 10b).

Although all the tributary canyons of the western set are prominent, the chirp data shows that some of them are being infilled while others are not (Fig. 8a). This indicates that downslope sediment transportation through the tributary canyons is an ongoing process but that these transportations are unevenly distributed over the tributary canyon system.

The eastern tributary canyon set is less prominent (Fig. 9). There, the individual canyons have widths and depths varying

between 1500 to 6000 m and 50 to 400 m, respectively (Fig. 9f).

The dimensions of individual canyons in both tributary canyon sets tend to decrease towards Kvitøya TMF (Figs 9d and 9f), where they gradually transit into significantly smaller, more linear gullies without tributaries that are superimposing Kvitøya TMF (Figs 10a-10b). These gullies lead down to the debris flow deposits and/or channel-levee deposits on the continental rise which may indicate that the channel-levee deposits are dominating the deposits there (Fig. 9a).

The differences in dimensions and development of the gullies is likely due to that the gullies off Kvitøya Trough more regularly are infilled by glacial sediments from Kvitøya Trough compared to the gully sets flanking them, which can form over longer time spans less affected by glacial infill (Figs 9-10).

Multibeam-backscatter strength is variable within the tributary canyons (Fig. 9c). The upper parts of the tributary canyons have values around -25 to -30 dB, which gradually increase to -20 dB in their lower parts (Fig. 9c). A bulge-shaped sediment deposit with strong multibeam-backscatter values of -20 to -30 dB is present below the western tributary canyon set at the continental rise (Fig. 9c). The location of the bulge-shaped sediment deposit indicates that it is a submarine fan formed by

repeated sediment delivery bypassing through the tributary canyons (c.f. Covault, 2011).

The areas unaffected by canyon erosion on the western flank of Kvitøya TMF are covered by acoustic unit C6, and normally display backscatter values of -30 to -40 dB (Fig. 8a). The higher backscatter values in the tributary canyons compared to their surroundings suggest that the tributary canyon areas consist of coarser sediments, which most likely result from erosion during active downslope sediment transport (Fig. 9c).

#### **6.4 Sediment mound and flanking channel**

A sediment mound is located on the middle continental slope at water depths between 730 and 1100 m (Fig. 10a). The mound extends beyond the seaward limit of the multibeam dataset used in this study; however, the part of the mound that we have mapped has the approximate dimensions of 22×15×0.2 km (Fig. 10a). Chirp data indicate that the sediment mound consists of acoustic unit C6, interpreted as layered glacimarine deposits (Fig. 10a). Subtle ridges are hinted at the acoustic basement of the sediment mound, however, these ridges are not visible on the overlying sea floor (Fig. 8a). The bathymetric data also show that the western tributary canyon set is incising the sediment mound, possibly via retrogressive upslope progression of gullies (Fig. 10a). The top of the sediment mound is characterized by a series of subtle, parallel to sub-

parallel linear ridges and troughs with wavelengths of approximately 500 m, amplitudes of 10-20 m, and SW-NE orientations (Fig. 10c). It is uncertain if the ridges in the bathymetry are related to the ridges hinted in the underlying chirp data since those ridges only appear under below the sea bed (Fig. 8a). A flat-bottomed channel with approximate dimensions of 10×4×0.1 km flanks the eastern side of the sediment mound (Fig. 10a). The channel extends down the upper slope and ends on the middle slope where smaller gullies connect to one of the larger tributary canyons (labelled in Fig. 10a and 10c).

## 7. Discussion

### *7.1. Variations in shelf-edge and slope morphology and architecture*

Our results indicate that the Albertini glacial trough-slope system is different from most other glacial troughs around Svalbard and the Barents Sea in several ways. Firstly, the mouth of Albertini Trough cuts back into the shelf edge, rather than protruding seaward, and does not have a TMF at the shelf edge and on the slope despite the fact that previous studies show prograding Quaternary sediments in the trough (Figs. 1; 11) (Geissler and Jokat 2004). Secondly, the morphology and sedimentology of the continental slope beyond Albertini Trough is dominated by thick, acoustically stratified units

instead of debris-flow deposits, which are typically the main building blocks of TMFs (Figs. 5; 8a) (e.g. Laberg and Vorren, 1995; Ó Cofaigh et al., 2003). Thirdly, the slope beyond Albertini Trough is characterised by a well-developed set tributary canyons incising the sea floor (Figs. 5c-d, 8a).

However, unlike Albertini Trough, the neighbouring Kvitøya Trough mouth does have a TMF that is depth-correlated to prograding Quaternary sediments (Fig. 3a). Although the deeper internal architecture of this fan is not as well imaged, the chirp and multibeam-backscatter data indicate that the sedimentology of the continental slope adjacent to Kvitøya Trough consists of coarse-grained glacial sediments (Figs 8b and 9c). The surface of the fan is relatively smooth but is incised by gullies significantly smaller and less developed than the tributary canyon sets flanking the trough mouth fan (Figs 9a-9b). Further down-slope, the continental rise and lower slope are covered by debris-flow and/or channel-levee deposits (Fig. 11).

The differences between the Albertini and Kvitøya glacial trough-slope systems can be explained by several factors. Firstly, the structural-geological setting of the two troughs differs considerably. Deep seismic-reflection profiles reveal that the acoustic basement below Albertini Trough is heavily down-faulted and lies between 2.5-3.5 sec TWT (1.9-2.6 km)

(Fig. 3) (Geissler and Jokat, 2004). The acoustic basement below Kvitøya Trough lies between 1.0-2.5 sec TWT (0.75-1.9 km) and is more intact, with significantly less throw on down-faulted sections (Fig. 3) (Geissler and Jokat, 2004). We suggest that the down-faulted bedrock surface below Albertini Trough provided a significantly larger accommodation space for the Late Pliocene sediments compared to the bedrock below Kvitøya Trough. Therefore, glacigenic sediments brought to the shelf edge by ice streaming through Albertini Trough probably filled the comparatively large accommodation space available instead of accumulating on, and building out onto the adjacent slope. We suggest that this is the reason for the absence of a significant trough-mouth fan deposit beyond Albertini Trough. The absence of a TMF beyond Albertini Trough probably facilitated tributary canyon incision which uninhibited of infill of glacigenic sediments could develop better than off Kvitøya Trough (Fig. 9a).

Secondly, we consider the sedimentary architecture of the continental slope beyond Albertini and Kvitøya troughs in order to determine the different sedimentation processes that may have shaped these margins.

The thick stratified units imaged by the airgun units A1-A4 from the middle to lower continental slope as well as by chirp (Unit C6) indicate that the dominant processes on the middle to

lower slope beyond Albertini Trough were deposition by contour currents and/or down-slope turbidity currents since the late Pliocene (Figs. 5; 8a). The continuous sequence of these units indicates that these processes also prevailed on the middle to lower continental slope during Quaternary. We suggest that this is due to relatively low input of glaciogenic sediments from Albertini Trough to the slope because those sediments were “trapped” in the accommodation space on the outer shelf (Figs. 3, 11). The slide scar on the middle continental slope in units A1 and A2 indicates that a mass-wasting event evacuated c. 0.3 sec TWT of late Pliocene-lower Quaternary sediments down the continental slope off Albertini Trough (Figs 5d and 10). The lobe-shaped sediment deposit adjacent to the slide scar is likely the depositional area for parts of the evacuated sediments from the slide scar (Figs. 10; 11). It is unlikely that this slope failure itself contributed to the cut-back of Albertini Trough into the shelf edge.

The recent deposition of acoustically laminated sediments (unit C6) and a sediment mound with superimposed sediment waves on the middle slope (Figs. 8a; 10) support the interpretation that the area is influenced strongly by contour currents. We suggest that the contourites on the slope adjacent to Albertini Trough were formed by deposition from the Svalbard branch of the WSC which flows eastward along the northern margin of Svalbard (e.g. Slubowska et al., 2005). Similar contourite drifts

formed by the WSC have been reported from the western Svalbard margin at water depths between 1200 and 1800 m (Rebesco et al., 2013), which covers the depth range of the contourites here (Figs. 8a; 10).

The semi-parallel internal reflectors of the Quaternary sediments covered by units A3 and A4 indicate that the stratigraphy of the upper slope off Albertini Trough was formed in a sedimentary environment influenced by both suspension settling and by gravity driven processes. This is supported by the chirp stratigraphy of the upper slope, indicating gravity driven processes during the maximum extent of the SBIS (Chauhan et al., 2016a). The lack of contourites on the upper slope may indicate the absence of contour currents here, unlike on the middle to lower slope (Fig. 8a).

The multibeam-backscatter and chirp data suggest that the flanks of Kvitøya TMF as well as the slope beyond Albertini Trough were heavily eroded by tributary canyon formation (Figs. 9c; 11). These tributary canyons likely developed during a relatively long time, since they are not filled in by glacial sediments derived from the shelf edge. We note that the similar location of the tributary canyons and the contourites could mean that the fine fraction of the debris flows entered the

nepheloid layer of the WSC, thus contributing to contourite formation along the northern continental slope (c.f. Rebesco et al., 2013).

The high multibeam-backscatter signals of the tributary canyons are suggested to come from relatively coarse-grained deposits from sediment-laden meltwater that eroded the tributary canyons on the continental slope during deglaciation (Fig. 9c) (c.f. Dowdeswell et al., 2006). The high multibeam-backscatter of the submarine fan on the continental rise adjacent to the western gully system indicates a depocentre for a substantial amount of the coarse-grained sediment that bypassed the gullies (Fig. 9c).

The sediment core PS2138-1, acquired from the continental slope adjacent to the eastern gully system at 995 m water depth contains a significant amount of terrigenous organic matter (TOM) (Fig. 1b) (Knies and Stein, 1998). The TOM was interpreted to have sourced from glacial sediments that bypassed the slope during the last deglaciation (Knies and Stein, 1998). The high TOM concentration supports the interpretation that down-slope gravity flows triggered by sediment-laden meltwater contributed to the erosion of the tributary canyons during deglaciation.

One of the major tributary canyons off Albertini Trough begins at the location of the previously mentioned slide scar, which

may indicate that the comparatively steep dip of the slide scar facilitated canyon formation from there (Fig. 10). This would also explain the absence of a major sediment deposit below the western to central slide scar, which likely was eroded by the canyon incision and brought to the continental rise (Fig. 10).

The significant dimension differences between the western and eastern tributary canyon sets suggest that a greater volume of material has bypassed the western gully set (Fig. 9). The channel on the upper slope beyond Albertini Trough is interpreted to have been eroded by a focused down-slope gravity flow from the shelf edge; the channel transitions into gullies connecting to the tributary canyon system where the slope gradient increases to  $>4^\circ$  (Figs 1; 10). We suggest that the focused gravity flows originating from the channel contributed significantly to the development of the larger western tributary canyon set (Figs. 9; 11). Furthermore, the transition from a channel to gullies at  $>4^\circ$  indicates that the erosive energy of the sediment-laden meltwater increased with increasing slope gradient, and that  $4^\circ$  is the minimum angle for gully erosion on this margin (Figs. 9-11).

Beyond Kvitøya Trough, the debris-flow and/or channel-levee deposits with a chaotic reflector pattern indicate that glacigenic sediments delivered from ice streaming through Kvitøya

Trough bypassed the relatively steep continental slope and accumulated as stacked deposits on the continental rise (Figs. 6; 8b; 9). The accumulation of debris-flow and/or channel-levee deposits is supported by the comparatively high multibeam-backscatter values of the hummocky terrain on the continental rise (Fig. 9c), implying comparatively coarse-grained glacial sediments there. We suggest that both debris-flows and gullies eroding the continental slope off Kvitøya Trough likely were facilitated by relatively steep upper-slope gradients ( $<9^\circ$ ), which yielded an unstable depositional environment for the glacial sediments. Previous research has suggested that TMF development is favored by slope gradients  $<1^\circ$  (Ó Cofaigh et al., 2003), which lends support to our interpretation. The comparatively small, less developed gullies incising Kvitøya TMF indicate that they formed after LGM since they otherwise likely would be covered by glacial sediments from Kvitøya trough mouth (Fig. 11).

The iceberg ploughmarks on the continental shelf edge indicate that calving was important for mass-loss during the last deglaciation of the northern Svalbard margin (Fig. 9b; 11). The larger ploughmarks on the upper continental slope have previously been suggested to originate from icebergs calving from large ice streams further eastward, such as in St. Anna and Franz Victoria Troughs (Fig. 11) (Dowdeswell et al., 2010; Dowdeswell and Hogan, 2016). Abundant smaller iceberg

ploughmarks have also been identified in Albertini Trough as well as from the inner continental shelf north of Nordaustlandet (Noormets et al., 2012; Fransner et al., in review).

### *7.2 Comparison to other troughs*

Kvitøya Trough and its associated TMF and catchment area have smaller dimensions compared to several cross-shelf troughs along the western Barents Sea (Fig. 2 and Table 3). This could indicate that ice in Kvitøya Trough was only of moderate importance for the drainage of the SBIS when compared with other ice streams (Fig. 2 and Table 3). Previous work has suggested that the full-glacial drainage basin for the Kvitøya Trough ice stream was relatively small, based on the sparse landform record and the relatively low elongation ratios of the landforms further south in Kvitøya Trough (Hogan et al., 2010). However, when comparing the TMFs of the Barents Sea region, it is evident that the bedrock of the western Barents Sea is dominated by sedimentary rocks of relatively low erosional resistivity whereas the bedrock of the northern margin is dominated by crystalline rocks (Elverhøi and Lauritzen, 1984). Therefore, the relatively high resistance to glacial erosion of the bedrock of Kvitøya Trough probably minimized the erosion rate of the streaming ice (Hogan et al., 2010). This lower erosion rate consequently reduced the volume of the trough as well as the volume of sediments delivered to its mouth (Table 3; Hogan et al., 2010).

The dimensions of Kvitøya Trough and its estimated drainage basin are similar to those of Hinlopen Trough, which is also located on the northern Svalbard margin (Fig. 2 and Table 3). In addition to these similarities, the bedrock geology is likely to be similar which makes a comparison between Kvitøya and Hinlopen troughs relevant (Hogan et al., 2010; Batchelor et al. 2011). Despite the similarities, Kvitøya Trough has a significantly larger TMF (Fig. 2 and Table 3). However, unlike Kvitøya, the slope beyond Hinlopen Trough has undergone a significant mass-wasting event, the Hinlopen-Yermak Slide, where  $1350 \text{ km}^3$  of sediments were evacuated to the Nansen Basin about 30,000 years ago (Vanneste et al., 2006; Winkelmann et al., 2008; Hogan et al., 2013). It is likely that most of the evacuated sediments are remnants of the Hinlopen TMF (Vanneste et al., 2006; Winkelmann et al., 2008). If the volume of the slide deposits is included in the estimation, the volume of Hinlopen TMF becomes c.  $1363.5 \text{ km}^3$ , which is similar to the estimated volume of the Kvitøya TMF. The similar volumes of the TMFs in similar geological settings may indicate similar drainage basin sizes and ice dynamics in the Kvitøya and Hinlopen troughs during Quaternary glacials.

The dimensions of Albertini Trough and its associated catchment area are significantly smaller compared to the neighboring Hinlopen and Kvitøya troughs (Fig. 2 and Table 3). These differences in size suggest that Albertini Trough is

less developed than the other two troughs, further indicating that less glacial sediments were brought to the slope through Albertini Trough (Fig. 2 and Table 3). A similar interpretation was made for the Mackenzie Trough system in the Canadian Arctic, which lacks a TMF, unlike its better-developed neighbouring Amundsen Gulf and M'Clure Strait Troughs (Fig. 2) (Batchelor et al., 2013). Our results suggest that although Albertini Trough seems to be less developed than Hinlopen and Kvitøya troughs, a proportionally sized TMF would be possible off Albertini Trough. However, the volume of Quaternary deposits in the area of the downfaulted bedrock below Albertini Trough mouth is of the same magnitude as the estimated volume of the Kvitøya TMF. The estimated volumes of Quaternary deposits support the idea that downfaulted bedrock below Albertini Trough mouth acted as a significant accommodation space for glacial sediments, with accumulation here thus preventing the build-up of a TMF on the slope (Fig. 12). Therefore, at Albertini Trough the evolution of the continental margin was controlled by pre-existing bedrock structure rather than sediment delivery; this example shows how a high-latitude continental margin can become dominated by erosional rather than depositional processes. Based on these findings we have developed a new schematic model for explaining the lack of a TMF (Fig. 12).

## 8. Conclusions

Based on the combined analysis of acoustic stratigraphy and seafloor bathymetry we have investigated the architecture and evolution of two glacial trough-continental slope systems on the northern Barents Sea margin (Fig. 1). We have identified the dominant Quaternary sedimentary processes acting in these two systems and the glaciological and geological factors affecting them. Our main findings are as follows.

- The shelf edge and continental slope beyond Kvitøya Trough is outward-bulging as a result of the buildup of a glacial TMF whereas the shelf edge and slope beyond of the adjacent Albertini Trough is incised and lacks a TMF.
- The main factor preventing the build-up of a TMF was the locally downfaulted bedrock below Albertini Trough, which yielded a larger accommodation space into which glacial sediments were deposited.
- A slide scar that formed in late Pliocene-early Pleistocene sediments on the middle continental slope indicates a mass-wasting event where c. 0.3 sec TWT of sediments were evacuated down-slope off Albertini Trough. Although this event likely did not contribute to the withdrawn trough mouth, the steep slide scar

became a start point for one of the major tributary canyons.

- The tributary canyons are flanking the sides of the Kvitøya TMF. The absence of glacial sediments facilitated the development of these tributary canyons which otherwise likely would have been buried or partly infilled.
- Beyond Kvitøya Trough, the relatively steep slope gradient caused the majority of the Quaternary TMF deposits to bypass the upper slope and reach the continental rise as debris-flows and/or through gullies forming channel-levee deposits. The Kvitøya TMF is incised by gullies suggesting that the gullies were active after the LGM, possibly as a consequence of sediment-laden meltwater triggering down-slope gravity flows that bypassed the slope and accumulated on the continental rise.
- Low slope gradients on the upper continental slope in front of both troughs limited the energy of the down-slope gravity flows, which prevented gully and canyon formation at the shelf edge.
- The Kvitøya TMF is significantly smaller than the TMFs of the western Barents Sea region, which we suggest is due mainly to the more erosion-resistant bedrock of the northern Barents Sea shelf, combined

with a relatively small interior ice-drainage basin when compared to drainage basins of ice streams that drained westwards from the Barents Sea (Table 1).

### **Acknowledgements**

This research has received funding from the People Programme (Marie Curie Actions) of the European Union's Seventh Framework Programme FP7/2007-2013/ under REA grant agreement n° 317217. The research forms part of the GLANAM (GLAciated North Atlantic Margins) Initial Training Network. The crew on R/V *Helmer Hanssen* is acknowledged for the data acquisition assistance. Multibeam-bathymetric data acquired during cruise JR142 of the RRS *James Clark Ross* was funded through UK Natural Environment Research Council grant NER/T/S/2003/00318 to JAD. Thanks to Martin Wikmar and Robin Dymind at Clinton Marine Survey, Gothenburg, who let me use their facilities during the completion of this work.

### **References**

Andreassen, K., Laberg, J. S., Vorren, T. O., 2008. Seafloor geomorphology of the SW Barents Sea and its glaci-dynamic implications. *Geomorphology* 97, 157-177.

Batchelor, C.L., Dowdeswell, J.A., Hogan, K.A., 2011. Late Quaternary ice flow and sediment delivery through Hinlopen

Trough, Northern Svalbard margin: Submarine landforms and depositional fan. *Marine Geology* 284, 13-27.

Batchelor, C.L., Dowdeswell, J.A., Pietras, J.T. 2013. Seismic stratigraphy, sedimentary architecture and palaeo-glaciology of the Mackenzie Trough: evidence for two Quaternary ice advances and limited fan development on the western Canadian Beaufort Sea margin. *Quaternary Science Reviews* 65, 73-87.

Batchelor, C.I., Dowdeswell, J.A., 2014. The physiography of high Arctic cross-shelf troughs. *Quaternary Science Reviews* 92, 68-96.

Cai, J., Powell, R.D., Cowan, E.A., Carlson, P.R. 1997. Lithofacies and seismic-reflection interpretation of temperate glacimarine sedimentation in Tarr Inlet, Glacier Bay, Alaska. *Marine Geology* 143, 5-37.

Chauhan, T., Rasmussen, T.L., Noormets, R., 2016a. Palaeoceanography of the Barents Sea continental margin, north of Nordaustlandet, Svalbard, during the last 74 ka. *Boreas* 45, 76-99.

Chauhan, T., Noormets, R., Rasmussen, T. L. 2016b. Glaciomarine sedimentation and bottom current activity on the north-western and northern continental margins of Svalbard during the late Quaternary. *Geo-Marine Letters* 36, 81-99.

Covault, J.A., 2011. Submarine fans and canyon-channel systems: A review of processes, products, and models. *Nature Education Knowledge* 3, 4.

Doré, A.G., 1995. Barents Sea Geology, Petroleum Resources and Commercial Potential. *Arctic* 48, 207-221.

Dowdeswell, J.A. and Hogan, K.A., 2016. Huge iceberg ploughmarks and associated corrugation ridges on the northern Svalbard shelf. *In* Dowdeswell, J.A. et al., (eds), *Atlas of Submarine Glacial Landforms: Modern, Quaternary and Ancient*. Geological Society, London, *Memoirs*, 46, 269-270.

Dowdeswell, J.A., Evans, J., Cofaigh, C.Ó., Anderson, J.B., 2006. Morphology and sedimentary processes on the continental slope off the Pine Island Bay, Amundsen Sea, West Antarctica. *Geological Society of America Bulletin* 118, 606-619.

Dowdeswell, J.A., Jakobsson, M., Hogan, K.A., O'Regan, M., Backman, J., Evans, J., Hell, B., Löwemark, L., Marcussen, C., Noormets, R., Cofaigh, C.Ó., Sellén, E & Sølvssten, M., 2010. High-resolution geophysical observations of the Yermak Plateau and northern Svalbard margin: Implications for ice-

sheet grounding and deep-keeled icebergs. *Quaternary Science Reviews* 29, 3518-3531.

Elverhøi, A., Lauritzen, Ø, 1984. Bedrock Geology of the Northern Barents Sea (West of 35° E) as inferred from the overlying Quaternary deposits *Norsk Polarinstitutt Skrifter* 180, 5-16.

Elverhøi, A., Pfirman, S.L., Solheim, A., Larssen, B.B., 1989. Glaciomarine sedimentation in epicontinental seas exemplified by the Northern Barents Sea. *Marine Geology* 85, 225-250.

Elverhøi, A., Norem, H., Andersen, E.S., Dowdeswell, J.A., Fossen, I., Haflidason, H., Kenyon, N.H., Laberg, J.S., King, E.L., Sejrup, H.P., Solheim, A., Vorren, T., 1997. On the origin and flow behaviour of submarine slides on deep sea fans along the Norwegian-Barents Sea continental margin. *Geo-Marine Letters* 17, 119-125.

Faleide, J.I., Solheim, A., Fiedler, A., Hjelstuen, B.O., Andersen, E.S., Vanneste, K., 1996.

Late Cenozoic evolution of the western Barents Sea-Svalbard continental margin. *Global and Planetary Change* 12, 53-74.

Flink, A.E., Noormets, R., Fransner, O., Hogan, K.A., O'Regan, M., Jakobsson, M. 2017. Past ice flow in

Wahlenbergfjorden and its implications for late Quaternary ice sheet dynamics in northeastern Svalbard. *Quaternary Science Reviews* 163, 162-179.

Fransner, O., Noormets, R., Flink, A.E., Hogan, K.A., O'Regan, M., Jakobsson, M. 2017. Glacial landforms and their implications for glacier dynamics in the Rijpfjorden and Duvefjorden, northern Nordaustlandet, Svalbard. *Journal of Quaternary Science* 32, 437-455.

García, M., Dowdeswell, J. A., Ercilla, G., Jakobsson, M. 2012. Recent glacially influenced sedimentary processes on the East Greenland continental slope and deep Greenland Basin. *Quaternary Science Reviews* 49, 64-81.

Gee, D. G., Fossen, H., Henriksen, N., Higgins, A. K. (2008). From the early Paleozoic platforms of Baltica and Laurentia to the Caledonide Orogen of Scandinavia and Greenland. *Episodes* 31, 44-51.

Geissler, W.H., Jokat, W., 2004. A geophysical study of the northern Svalbard continental margin. *Geophysical Journal International* 158, 50-66.

Heafford, A.P., 1988. Carboniferous through Triassic stratigraphy of the Barents Shelf. In: Harland, W.B and

Dowdeswell E.K (eds.): Geological evolution of the Barents Shelf region, 89-108. Graham and Trotman, London.

Elverhøi, A., Lauritzen, Ø., 1984. Bedrock Geology of the Northern Barents Sea (West of 35° E) as inferred from the overlying Quaternary deposits Norsk Polarinstitutt Skrifter 180: 5-16.

Hjelstuen, B., Kjennbakken, H., Bleikli, V., Anthoni Ersland, R., Kvilhaug, S., Euler, C., Alvheim, S., 2013. Fjord stratigraphy and processes – evidence from the NE Atlantic Fensfjorden system. *Journal of Quaternary Science* 28, 421-432.

Hogan, K.A., Dowdeswell, J.A., Noormets, R., Evans, J., Ó Cofaigh, C., Jakobsson, M., 2010. Submarine landforms and ice-sheet flow in the Kvitøya Trough, northwestern Barents Sea. *Quaternary Science Reviews* 29, 3345-3562.

Hogan, K.A., Dix, J.K., Lloyd, J.M., Long, A.J., Cotterill, C.J., 2011. Seismic stratigraphy records the deglacial history of Jakobshavn Isbræ, West Greenland. *Journal of Quaternary Science* 26, 757-766.

Hogan, K.A., Dowdeswell, J.A., and Mienert, J., 2013. New insights into slide processes and seafloor geology revealed by

side-scan imagery of the massive Hinlopen Slide, Arctic Ocean margin. *Geo-Marine Letters*, 33, 325-343.

Hughes, A. L., Gyllencreutz, R., Lohne, Ø. S., Mangerud, J., Svendsen, J. I. 2016. The last Eurasian ice sheets—a chronological database and time-slice reconstruction, DATED-1. *Boreas* 45, 1-45.

Jakobsson, M., L. A. Mayer, B. Coakley, J. A. Dowdeswell, S. Forbes, B. Fridman, H. Hodnesdal, R. Noormets, R. Pedersen, M. Rebesco, H.-W. Schenke, Y. Zarayskaya A, D. Accettella, A. Armstrong, R. M. Anderson, P. Bienhoff, A. Camerlenghi, I. Church, M. Edwards, J. V. Gardner, J. K. Hall, B. Hell, O. B. Hestvik, Y. Kristoffersen, C. Marcussen, R. Mohammad, D. Mosher, S. V. Nghiem, M. T. Pedrosa, P. G. Travaglini, and P. Weatherall, The International Bathymetric Chart of the Arctic Ocean (IBCAO) Version 3.0, *Geophysical Research Letters*.

Kane, I.A., McCaffrey, W.D., Peakall, J., Kneller, B.C., 2010. Submarine channel levee shape and sediment waves from physical experiments. *Sedimentary Geology* 223, 75-85.

King, E.L., Haflidason, H., Sejrup, H.P., Løvlie, R., 1998. Glacigenic debris flows on the North Sea Trough Mouth Fan during ice stream maxima. *Marine Geology* 152, 217-246.

Knies, J., Stein, R., 1998. New aspects of organic carbon deposition and its paleoceanographic implications along the

Northern Barents Sea margin during the last 30000 years. *Paleoceanography* 13, 384-394.

Knies, J., Nowaczyk, N., Muller, C., Vogt, C., Stein, R., 2000. A multiproxy approach to reconstruct the environmental changes along the Eurasian continental margin over the last 150000 years. *Marine Geology* 163, 317-344.

Knies, J., Kleiber, H-P., Matthiessen, J., Muller, C., Nowaczyk, N., 2001. Marine ice-rafted debris records constrain maximum extent of Saalian and Weichselian ice-sheets along the northern Eurasian margin. *Global and Planetary Change* 31, 45-64.

Laberg, J. S., Vorren, T.O., 1995. Late Weichselian submarine debris flow deposits on the Bear Island TM Fan. *Marine Geology* 127, 45-72.

Laberg, J. S., Vorren, T.O., 1996. The glacier-fed fan at the mouth of Storfjorden trough, western Barents Sea: a comparative study. *Geologische Rundschau* 85, 338-349.

Mangerud, J., Dokken, T., Hebbeln, D., Heggen, B., Ingolfsson, O., Landvik, J.Y., Mejdahl, V., Svendsen, J.I., Vorren, T.O., 1998. Fluctuations of the Svalbard-Barents Sea ice sheet during the last 150000 years. *Quaternary Science Reviews* 17, 11-42.

Noormets, R., Hogan, K., Austin, W., Chauhan, T., Roy, S., Rasmussen, T., Dowdeswell, J., 2012. Submarine glacial

landform assemblages on the outer continental shelf north of Nordaustlandet, Svalbard. In: The 6th Arctic Paleoclimate and its Extremes (APEX) Meeting, Program and Abstracts, Oulu University, 15-18 May. Oululanka Research Station, Finland, p. 70.

O'Cofaigh, C., Taylor, J., Dowdeswell, J. A., Pudsey, C. J., 2003. Palaeo-ice streams, TM fans and high-latitude continental slope sedimentation. *Boreas* 32, 37–55.

Ottesen, D., Dowdeswell, J.A., Rise, L., 2005. Submarine landforms and the reconstruction of fast-flowing ice streams within a large Quaternary ice-sheet: The 2500-km-long Norwegian-Svalbard margin (57°-80°N). *Geological Society of America Bulletin* 117, 1033-1050.

Ottesen, D., Dowdeswell, J.A., Landvik, J.Y., Mienert, J., 2007. Dynamics of the Late Weichselian ice sheet on Svalbard inferred from high-resolution sea-floor morphology. *Boreas* 36, 286-306.

Ottesen, D., Dowdeswell, J.A., 2009. An inter-ice stream glaciated margin: submarine landforms and a geomorphic model based on marine-geophysical data from Svalbard. *Geological Society of America Bulletin* 121, 1647-1665.

Pudsey, C.J., 2000. Sedimentation on the continental rise west of the Antarctic Peninsula over the last three glacial cycles. *Marine Geology* 167, 313-338.

Rebesco, M., Larter, R.D., Camerlenghi, A., Barker, P.F., 1996. Giant sediment drifts on the continental rise west of the Antarctic Peninsula. *Geo-Marine Letters* 16, 65-75.

Rebesco, M., Wåhlin, A., Laberg, J.S., Schauer, U., Beszczynska-Möller, A., Lucchi, R.G., Noormets, R., Accettella, D., Zarayskaya, Y., Diviacco, P., 2013. Quaternary contourite drifts on the western Spitsbergen margin. *Deep Sea Research Part I: Oceanographic Research Papers* 79, 156-168.

Sarkar, S., Berndt, C., Chabert, A., Masson, D. G., Minshull, T. A., Westbrook, G. K. 2011. Switching of a paleo-ice stream in northwest Svalbard. *Quaternary Science Reviews* 30, 1710-1725.

Siegert, M.J., Dowdeswell, J.A., Hald, M., Svendsen, J.I. 2001. Modelling the Eurasian Ice Sheet through a full (Weichselian) glacial cycle. *Global and Planetary Change* 31, 367-385.

Slubowska, M.A., Koc, N., Rasmussen, T.L., Klitgaard-Kristensen, D., Changes in the flow of Atlantic water into the Arctic Ocean since the last deglaciation: evidence from the

northern Svalbard continental margin, 80°N. *Paleoceanography* 20, PA4014.

Svendsen, J.I., Alexanderson, H., Astakhov, V.I., Demidov, I., Dowdeswell, J.A., Funder, S., Gataullin, V., Henriksen, M., Hjort, C., Houmark-Nielsen, M., Hubberten, H.W., 2004. Late Quaternary ice sheet history of northern Eurasia. *Quaternary Science Reviews*, 23, 1229-1271.

Vanneste, M., Mienert, J., Bunz, S., 2006. The Hinlopen Slide: a giant, submarine slope failure on the northern Svalbard margin, Arctic Ocean. *Earth and Planetary Science Letters* 245, 373-388.

Vorren, T.O., Hald, M., Lebesbye, E., 1988. Late Cenozoic environments in the Barents Sea. *Paleoceanography* 3, 601–612.

Winkelmann, D., Geissler, W., Schneider, J., Stein, R., 2008. Dynamics and timing of the Hinlopen/Yermak megaslide north of Spitsbergen, Arctic Ocean. *Marine Geology* 250, 34-50.

Worsley, D., Aga, O., 1986. The geological history of Svalbard – Evolution of an Arctic archipelago. Statoil, Stavanger: 121 pp.

### **Figure and table captions**

Figure 1. (a) Location of study area on the outer continental shelf and slope north of Nordaustlandet, Svalbard. West Spitsbergen Current (WSC),

Yermak Branch (YB) and Svalbard Branch (SB) are arrowed and labeled. (b) Multibeam-bathymetric coverage (depth range 100 to 3000 m). The black dashed and solid lines show the location of the airgun and chirp profiles. The gravity core locations for PS2138-1 and HH11-09 (Knies and Stein, 1998; Chauhan et al., 2016a) are arrowed. The white dashed lines represent the likely extension of the Kvitøya TMF, based on the relatively rough bathymetry on the continental rise and the bulge-shape on the continental edge. The numbers in white (in km) indicate the depth range of the IBCAO map (Jakobsson et al., 2012). (c) Map showing the source of the three bathymetry datasets used (HH is from *Helmer Hanssen* and JCR is from *James Clark Ross*). (d) Seafloor profile of the continental slope seaward of Kvitøya Trough, which is concave with a maximum dip of  $9^\circ$ . (e) Seafloor profile of the slope adjacent to Albertini Trough with its convex shape and more variable slope gradients (max.  $4^\circ$  to 1000 m water depth, then  $12^\circ$ ); the arrow indicates the start of gullies on the slope.

Figure 2. (a) and (b) Location and approximate drainage area of Arctic troughs (red). The presence and absence of a locally bulge-shaped slope adjacent to these troughs are marked with yellow and black, respectively. (After Batchelor and Dowdeswell, 2014). The troughs mentioned in this paper are labelled. The dashed black line and the white line in Kvitøya and Albertini Troughs show the location of figures 3a and 3b. Regional bathymetry is from IBCAO 3.0 (Jakobsson et al., 2012).

Figure 3. (a) Interpretation of a seismic-reflection profile from Kvitøya Trough and adjacent continental slope (after Geissler and Jokat, 2004). The location of the profile is presented in Figure 2. The sediment thickness reaches from 0 sec TWT on the shelf to ca. 2.5 sec TWT (c. 0-1900 m) in Nansen Basin (after Geissler and Jokat, 2004). (b) Interpretation of a seismic-reflection profile from Albertini Trough and adjacent continental

slope (after Geissler and Jokat, 2004). The location of the profile is presented in Figure 2. The sediment thickness reaches from 0 sec TWT on the shelf to ca. 3 sec TWT (c. 2300 m) on the downfaulted upper continental slope and in Nansen Basin (after Geissler and Jokat, 2004). The black boxes and lines show the locations of the seismic-reflection profiles presented in figures 4-6.

Figure 4. (a) Seismic-reflection profile from the upper continental slope beyond Kvitøya Trough. (b) Interpretation of seismic profile in (a). The dashed reflector is a sea-floor multiple. The vertical “striping” artefacts in the seismic data are due to rough sea conditions during data acquisition. Location of the profile is shown in Figure 1.

Figure 5. (a) Seismic-reflection profile along the mouth of Albertini Trough. (b) Interpretation of the seismic profile in (a) shows that the imaged data cover c. 0.3 sec TWT and are subdivided into seismic units A1-A4. The dashed line is a sea-floor multiple. Location of the profile is shown in Figure 1. (c) Seismic profile along the middle continental slope beyond Albertini Trough. (d) Interpretation of the seismic profile in (c) shows that the imaged data cover c. 0.8 sec TWT and consist of seismic units A1-A4. The erosional boundary indicates a canyon cutting into the sediment stratigraphy (arrowed). A buried slide scar below the tributary canyons in the seabed cuts A1 and A2. Location of the profile is shown in Figure 1.

Figure 6. (a) Seismic-reflection profile along the continental rise. (b) Interpretation of the seismic profile in (a) shows data-coverage for the top 0.3 sec TWT and that this sediment has semi-parallel to chaotic reflector geometry. These sediments are of Quaternary age based on depth-correlation with Geissler and Jokat (2004) (Fig. 3). Location of the profile is shown in Figure 1.

Figure 7. (a) Chirp profile across the upper slope beyond Albertini Trough. (b) Interpretation of (a) showing relatively thick sediment cover consisting of C1-C5. The location and approximate penetration depth of gravity core HH11-09 (Chauhan et al., 2016a) is also shown. Location of the profile is shown in Figure 1.

Figure 8. (a) Chirp profile across the middle-lower continental slope off Albertini Trough where a tributary canyon network (arrowed) cuts through the uppermost units (C6) and erodes the side of a sediment mound. Subtle ridges are hinted at the base of the sediment mound. The large arrow is pointing to the tributary canyon shown in the seismic-reflection data (Fig. 4c). All the arrows are labeled with "Infill" or "no infill", which refers to that some tributary canyons are filled with sediments while others are not. (b) Chirp profile along the continental slope offshore of Kvitøya Trough, which is dominated by acoustic facies C1. (c) Blow-up of (b) shows two lobes of C8 on the lower continental slope. The respective location of the chirp profiles is shown in Figure 1.

Figure 9. (a) Multibeam-bathymetric data showing Kvitøya TMF with tributary canyon sets flanking its western and eastern sides. Smaller gullies generally extend from the upper to lower continental slope of the Kvitøya TMF where they connect to debris-flow-and/or channel levee deposits. (b) The shelf edge is heavily scoured by iceberg ploughmarks. (c) A multibeam-backscatter image of the slope, indicating that the TMF has stronger multibeam-backscatter than the flanking areas eroded by tributary canyon sets. The white dashed lines mark the boundaries between the TMF and the areas of the slope incised with tributary canyons. A submarine fan with relatively high multibeam-backscatter values (labeled) is present below the tributary canyon set west of the TMF. (d) Seafloor profile of the western

tributary gully set. (e) Seafloor profile of the Kvitøya TMF. (f) Seafloor profile of the eastern tributary canyon set.

Figure 10. (a) Continental slope of the western flank of Kvitøya TMF. The start of gullies is indicated at 1160 m water depth. A slide scar crossing the middle continental slope correlates with the beginning of the western gully set. A lobe-shaped sediment deposit associated with the eastern part of the slide scar is located east of the tributary canyons. A channel is found upslope of one of the tributary canyons. (b) A cross-profile covering one of the major tributary canyons and the lobe-shaped sediment deposit shows that the flanks of the lobe-shaped deposit are eroded by canyon and gully incision (c) A cross-profile shows that the channel is ca. 4 km wide and 50-100 m deep. The channel is cutting a sediment mound found to the west of the channel. The sediment mound is superimposed by sediment waves (arrowed).

Figure 11. Morphology of the outer shelf and slope north of Nordaustlandet, Svalbard. Kvitøya Trough mouth is bulging outwards and displays an adjacent TMF which Albertini Trough does not have. Instead, the slope beyond Albertini Trough is heavily incised by a tributary canyon set. The Kvitøya TMF extends down-slope beyond the dataset (Fig. 1).

Figure 12. Schematic model of Albertini Trough mouth suggesting that the downfaulted bedrock on the shelf edge acts as a trap for glacial sediment, preventing TMF development on the adjacent slope. The trapping of the glacial sediments facilitates canyon development over longer time spans compared to below troughs with associated TMFs.

Table 1. Seismic units A1-A5 identified from the seismic-reflection data from the continental slope of the study area. The unit examples are arrowed in each image.

Table 2. Acoustic units C1-C8 identified from the chirp data from the continental shelf edge and slope in the study area. The unit examples are arrowed in the table. The spikes in the data examples are heave artefacts (arrowed in Fig. 6).

Table 3. A selection of glacial cross-shelf troughs, their dimensions, approximate ice-stream drainage basins, shelf width, and approximate TMF volume (adapted from Batchelor and Dowdeswell, 2014). Albertini and Kvitøya troughs (above the first dotted line) are the focus of this study. Bear Island, Hinlopen and Storfjorden troughs are also situated on the Svalbard margin; the Mackenzie and Scoresby Sund troughs are from the Canadian and Greenland margins, respectively.

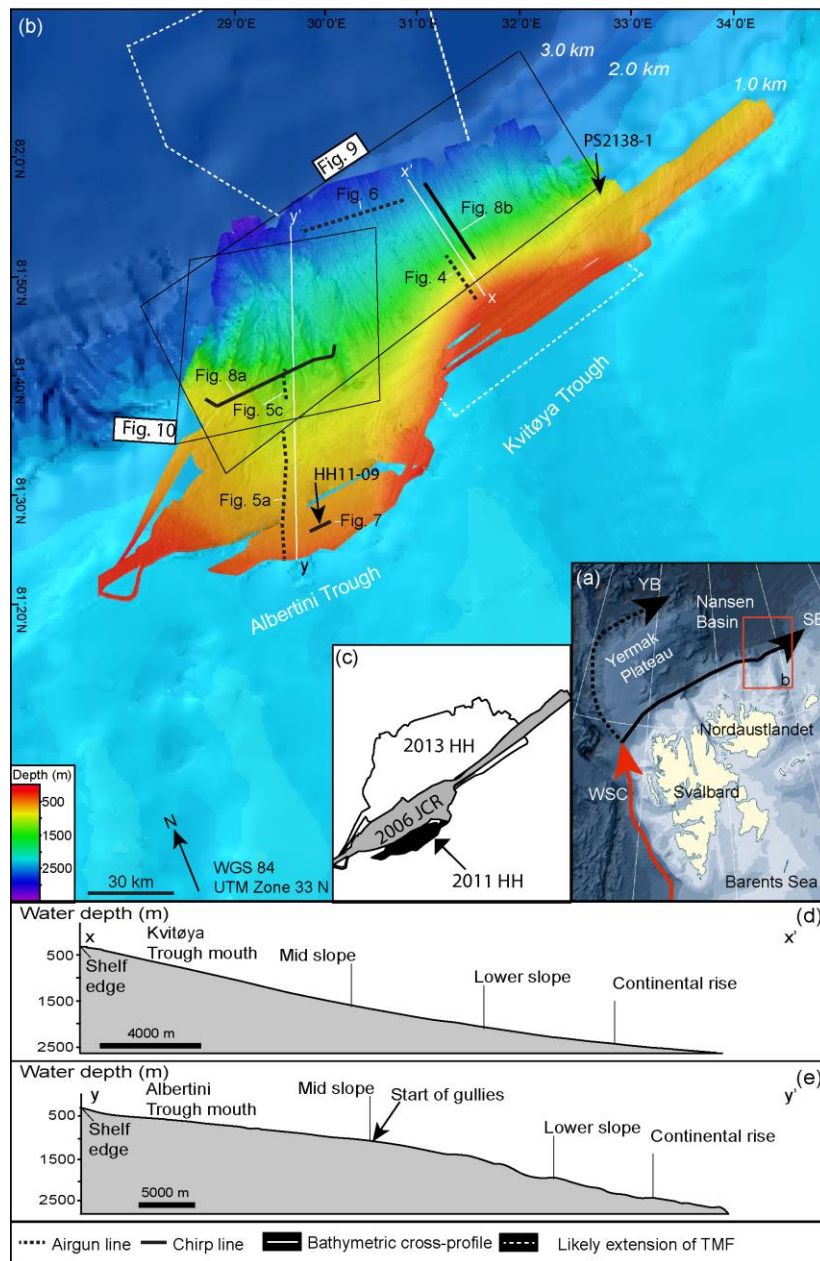


Figure 1

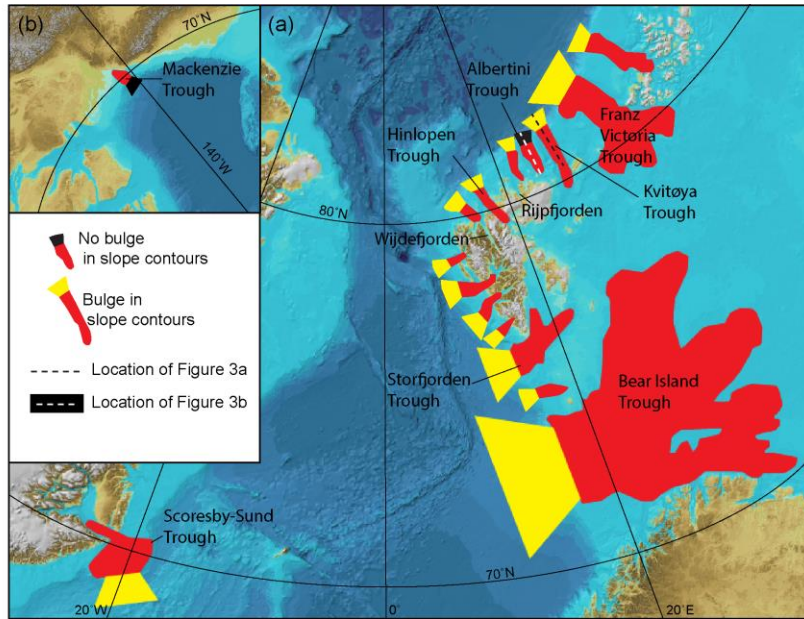


Figure 2

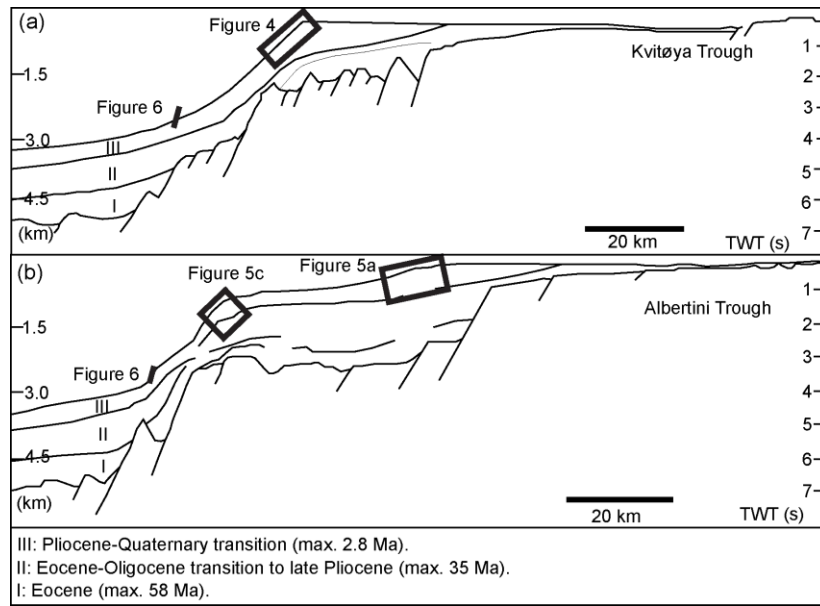


Figure 3

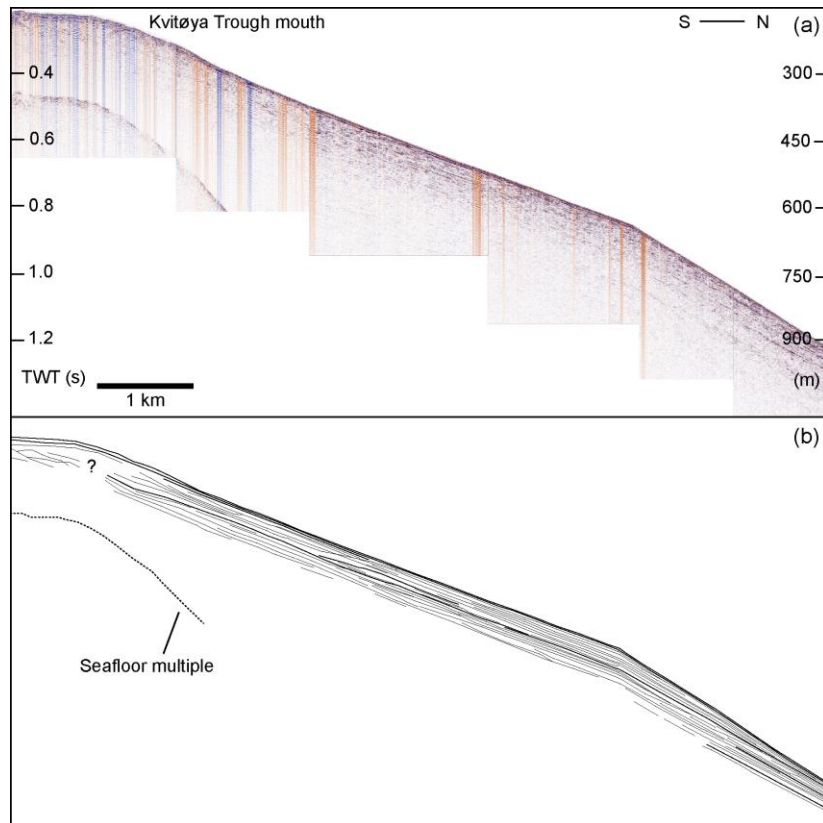


Figure 4

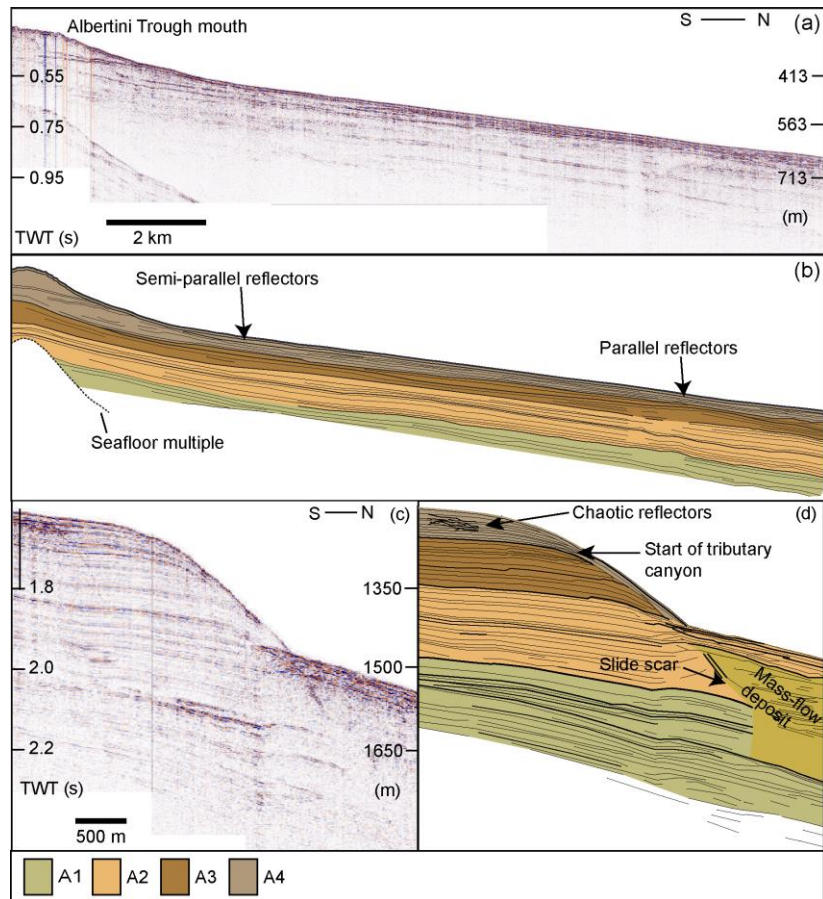


Figure 5

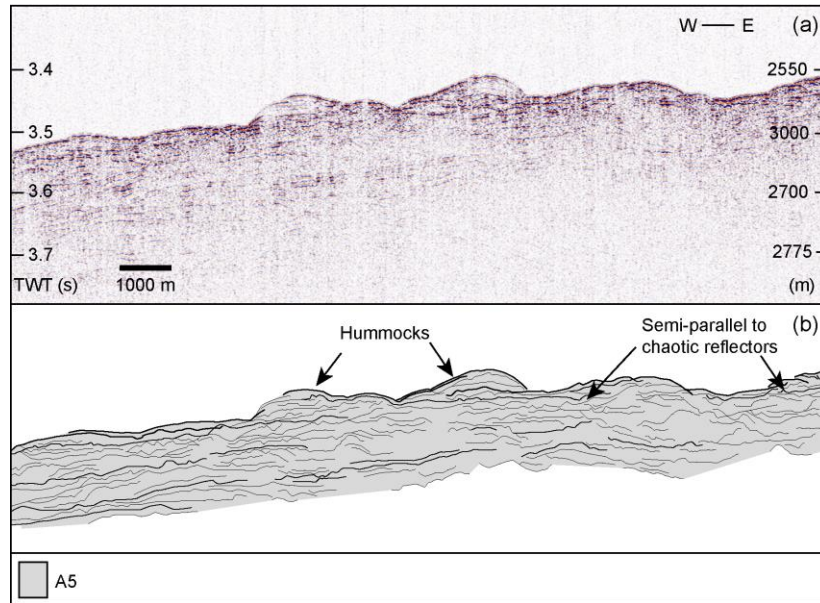


Figure 6

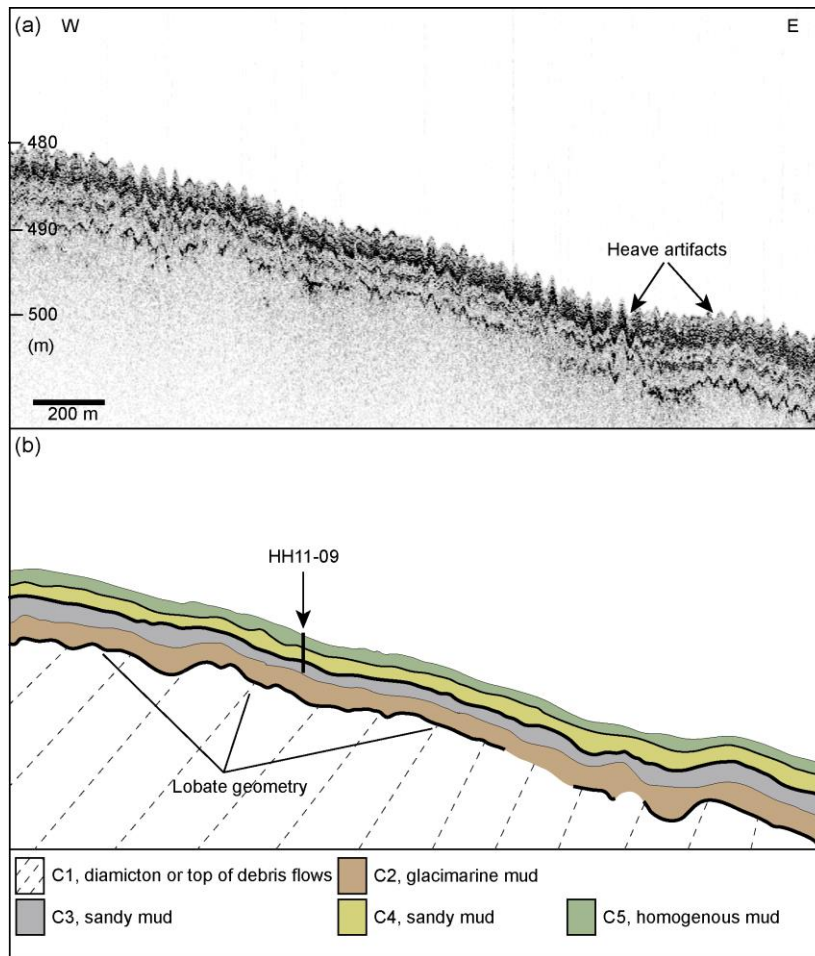


Figure 7

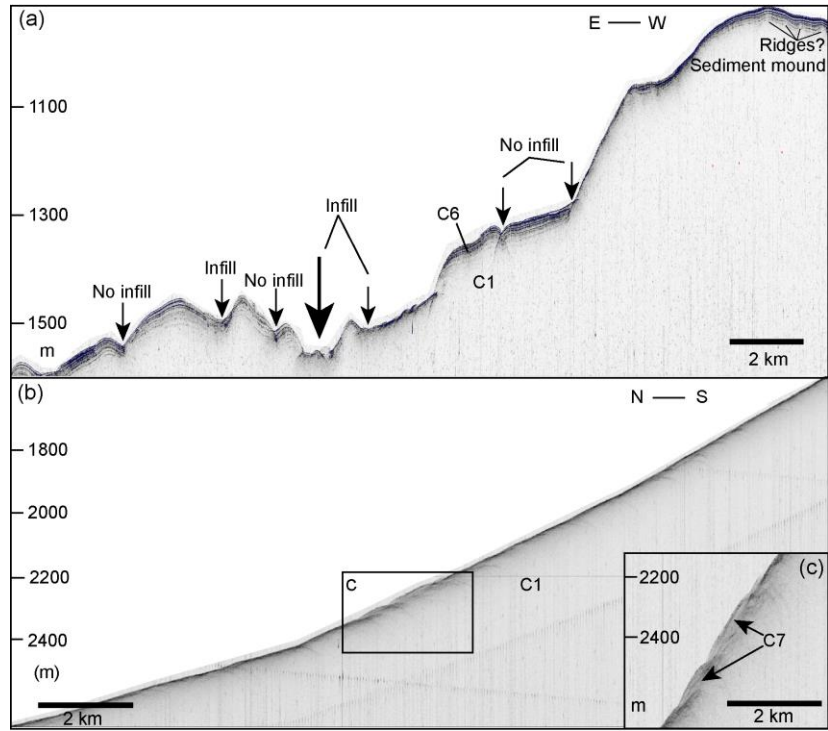


Figure 8

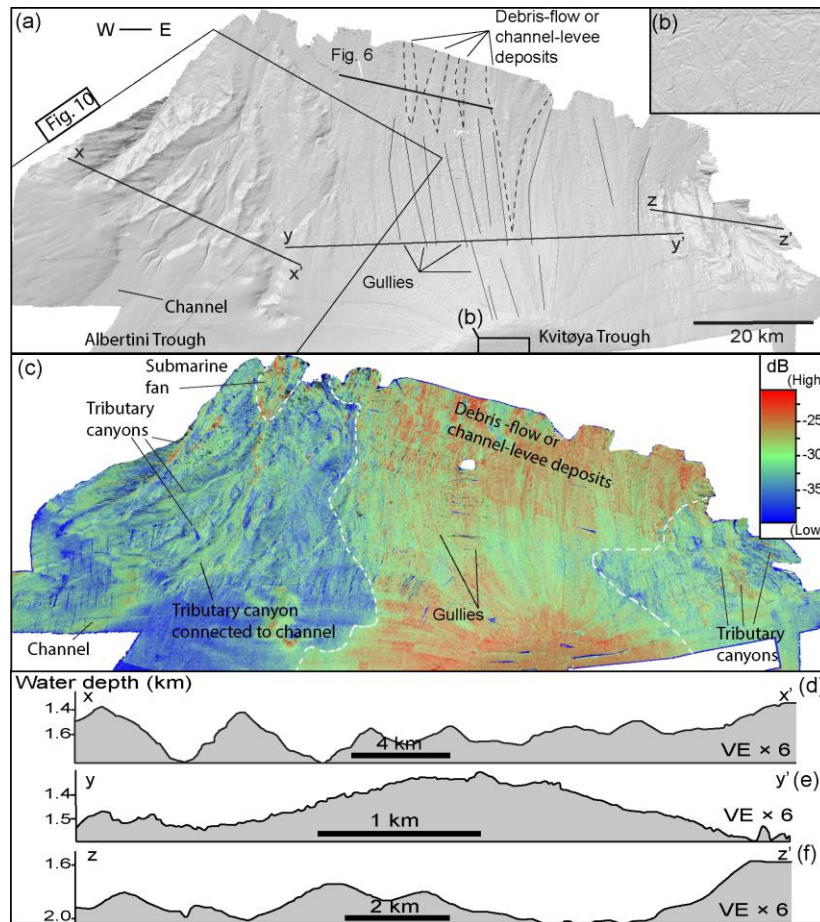


Figure 9

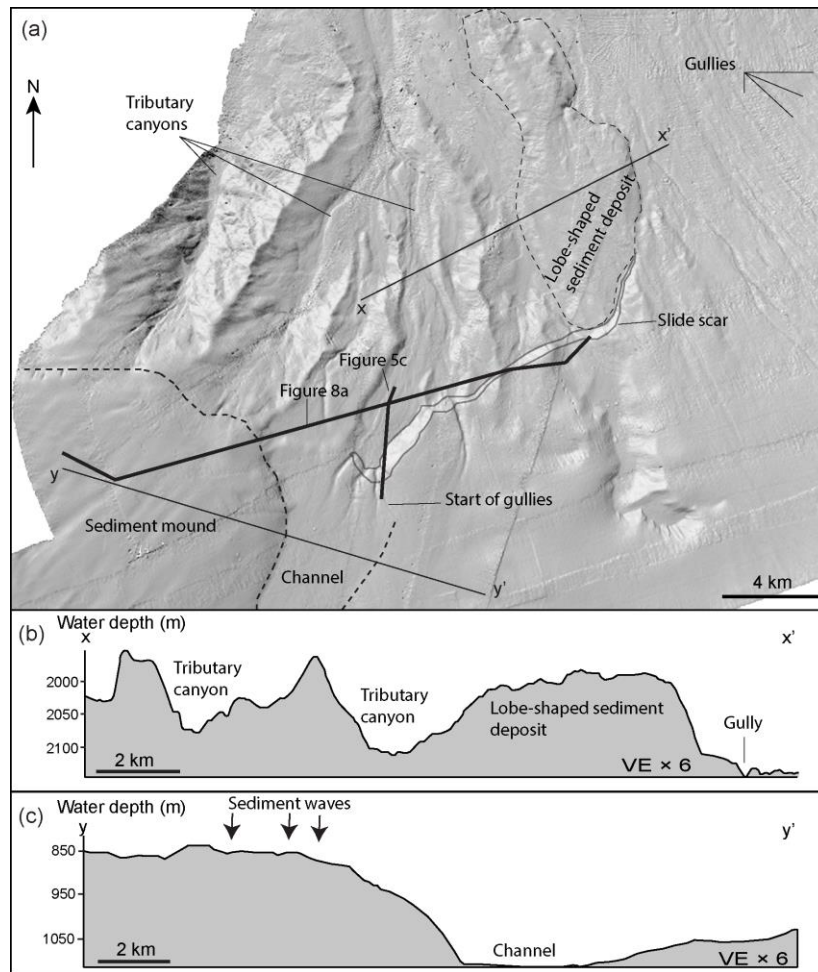


Figure 10

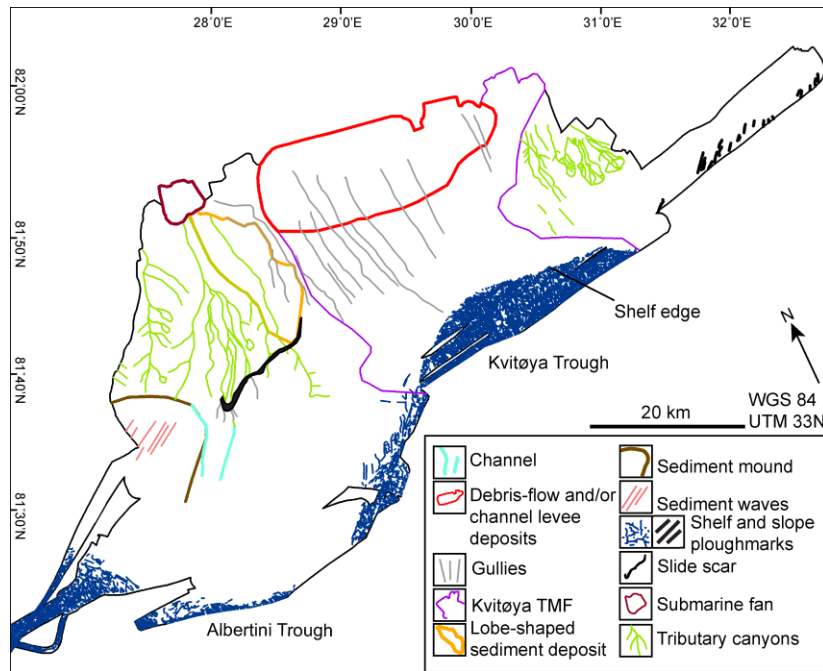


Figure 11

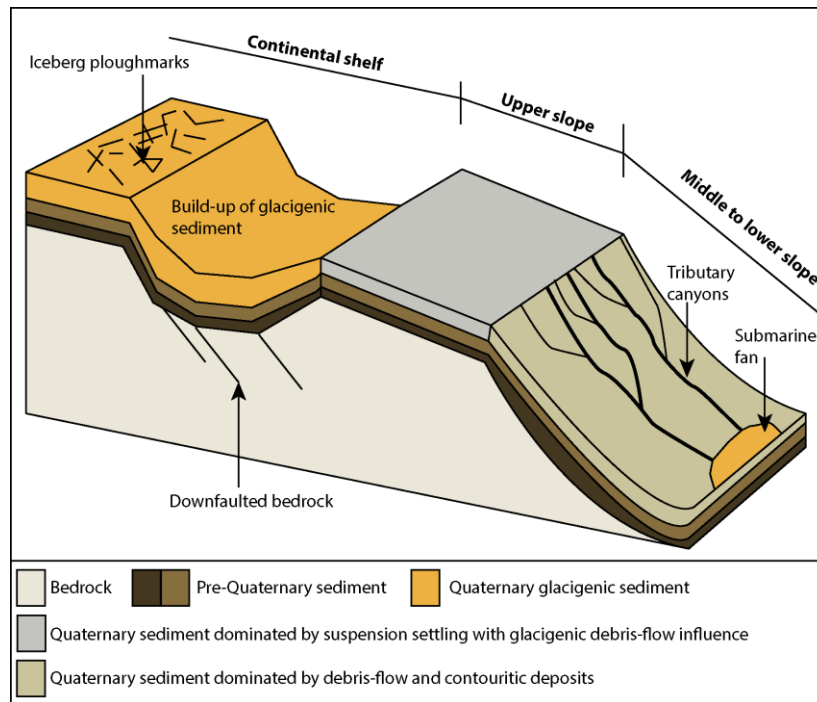
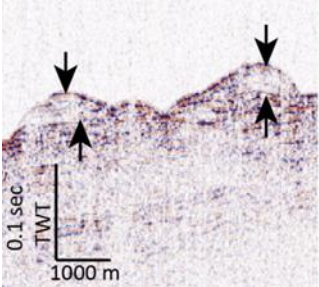
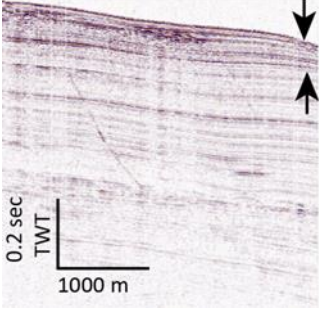
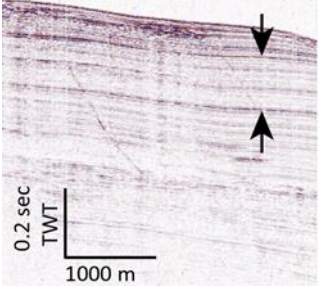
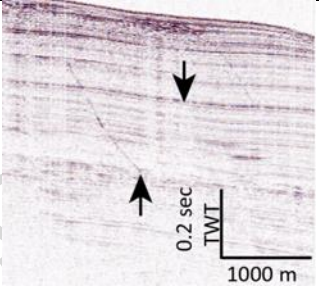
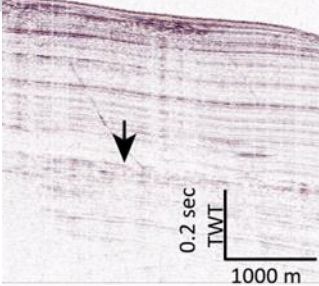
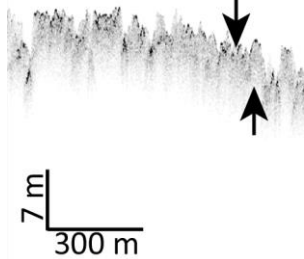
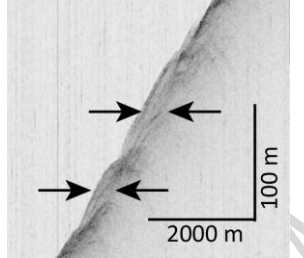
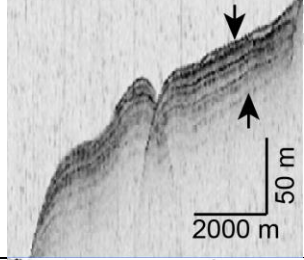
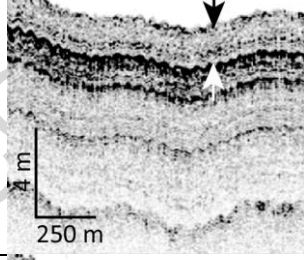
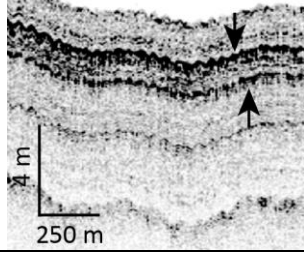


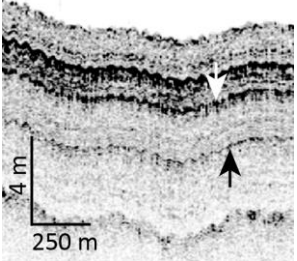
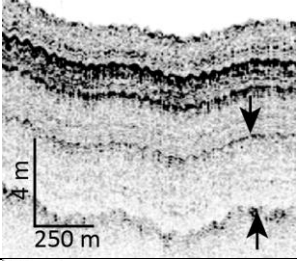
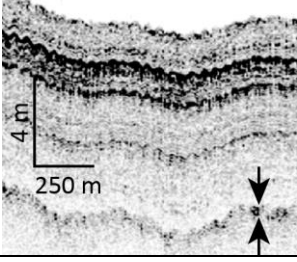
Figure 12

**Table 1:**

Unit	Data example	Description
A5		Moderate-high amplitude and high continuity of upper bounding reflector. Semi-parallel to chaotic reflection geometry. Locally present on the continental rise.
A4		High amplitude and continuity of upper bounding reflector. Internal, semi-parallel to parallel reflectors of high amplitude and continuity. Local high amplitude reflectors of chaotic pattern.
A3		High amplitude and high continuity of the upper bounding reflector. Internal reflectors of moderate amplitude and continuity. The reflectors are semi-parallel to parallel to each other.
A2		Moderate amplitude and high continuity of the upper bounding reflector. Internal reflectors of moderate amplitude and continuity. The reflectors are semi-parallel to parallel to each other.
A1		Low amplitude and moderate continuity of the upper bounding reflector. Internal reflectors of low amplitude and continuity. The reflectors are semi-parallel to parallel to each other.

**Table 2:**

Unit	Data example	Description
C8		Low-moderate amplitude and moderate continuity of the upper bounding reflector. Very little to no penetration. Undulating reflector due to ploughmarks.
C7		Acoustically transparent lobes. Moderate-high amplitude and medium continuity of the upper bounding reflector. Present at the continental slope and rise.
C6		High amplitude and continuity of the upper bounding reflector. Internal reflectors of high amplitude and continuity which are semi-parallel to parallel to each other.
C5		Moderate to high amplitude and high continuity of the upper bounding reflector. Locally internal, parallel reflectors of high amplitude and low-medium continuity.
C4		High amplitude and high continuity of the upper bounding reflector. Internal reflectors of high amplitude and low continuity. The reflectors are semi-parallel to parallel to each other.

<b>C3</b>		High amplitude and high continuity of the upper bounding reflector. Internal reflectors of low amplitude and low continuity. The reflectors are semi-parallel to parallel to each other.
<b>C2</b>		Moderate amplitude and moderate continuity of the upper bounding reflector. Acoustically transparent to semi-transparent unit.
<b>C1</b>		Moderate amplitude and moderate continuity of the upper bounding reflector. Constitutes the bounding reflector of the acoustic basement.

**Table 3:**

Trough	Trough length (km)	Trough width (km)	Trough depth (km)	App. ice-stream drainage basin (km <sup>2</sup> )	Shelf width (km)	App. volume of TMF (km <sup>3</sup> )
Albertini Kvitøya	100 190	35 25	0.22 0.5	6000 15000	110 190	No TMF 1000
Bear Island	700 180	260 22	0.5 0.43	500000 18000	700 70	35000 0
Hinlopen Storfjorden	250	125	0.42	60000	250	13.5 11600 0
Mackenzie Scoresbysund	180 480	70 150	0.4 0.6	250000 60000	180 130	No TMF 15000

**Highlights**

- The shelf edge and continental slope beyond Kvitøya Trough is outward-bulging as a result of the buildup of a glacial TMF whereas the shelf edge and slope beyond the adjacent Albertini Trough is incised and lacks a TMF.
- The main factor preventing the build-up of a TMF was the locally downfaulted bedrock below Albertini Trough, which yielded a larger accommodation space into which glacial sediments were deposited.